ASAR IMAGES A DIVERSE SET OF DEFORMATION PATTERNS AT KĪLAUEA VOLCANO, HAWAI`I

Michael P. Poland[(1)]

[(1)]*U.S. Geological Survey, Hawaiian Volcano Observatory, 51 Crater Rim Road, Hawai`i National Park, HI 96718-0051, U.S.A., Email: mpoland@usgs.gov*

ABSTRACT

Since 2003, 27 independent look angles have been acquired by ENVISAT's Advanced Synthetic Aperture Radar (ASAR) instrument over the island of Hawai`i, allowing for the formation of thousands of interferograms showing deformation of the ground surface. On Kīlauea volcano, a transition from minor to broad-scale summit inflation was observed by interferograms that span 2003 to 2006. In addition, radar interferometry (InSAR) observations of Kīlauea led to the discovery of several previously unknown areas of localized subsidence in the caldera and along the volcano's east rift zone. These features are probably caused by the cooling and contraction of accumulated lavas. After November 2005, a surface instability near the point that lava entered the ocean on the south flank of Kīlauea was observed in interferograms. The motion is most likely a result of unbuttressing of a portion of the coast following the collapse of a large lava delta in November 2005. InSAR data can also be used to map lava flow development over time, providing ~30 m spatial resolution maps at approximately monthly intervals. Future applications of InSAR to Kīlauea will probably result in more discoveries and insights, both as the style of volcano deformation changes and as data from new instruments are acquired.

1. INTRODUCTION

The Big Island of Hawai`i (Fig. 1) is home to three volcanoes that have erupted historically. Hualālai, on the east side of the island, last erupted in 1801 [1]. Mauna Loa, the largest volcano on the planet, has erupted 39 times since 1832, most recently in 1984 [2]. Kīlauea, which has been in a state of continuous eruption since 1983 [3], is one of the most active volcanoes in the world. Kīlauea (Fig. 1 zoomed panel) has been the focus of continuous observation and ongoing research since the 1912 founding of the Hawaiian Volcano Observatory, and deformation monitoring has played an important role in studying eruptive and intrusive activity there. Today, geodetic monitoring at Kīlauea includes both continuous and campaign Global Positioning System (GPS) measurements, continuous borehole tilt and strain measurements, leveling surveys, and radar interferometry (InSAR) measurements. Of these techniques, InSAR provides unparalleled spatial resolution of deformation, and its recent application to Kīlauea has provided important ground motion data for monitoring and hazard assessment purposes, as well as the discovery of several previously unknown deforming regions.

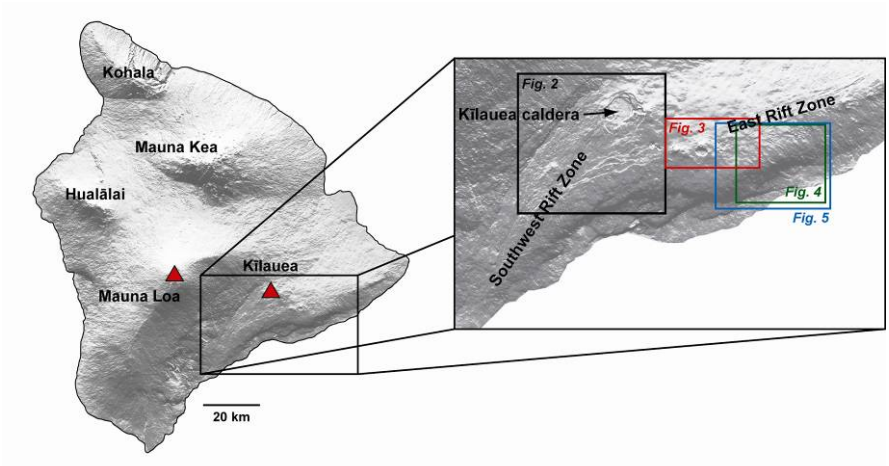

Figure 1. Map showing the locations of the major volcanic centers on the island of Hawai`i. The summit calderas of Mauna Loa and Kīlauea, the most active volcanoes on the island, are indicated by red triangles. Zoomed map shows the areas on Kīlauea covered by Figs. 2-5

Below, InSAR data obtained from Kīlauea volcano using ENVISAT's Advanced Synthetic Aperture Radar (ASAR) instrument are described. The results can be broadly categorized into 1) volcano-wide deformation,

2) localized subsidence due to lava accumulation, 3) surface instability, and 4) lava flow mapping.

2. VOLCANO-WIDE DEFORMATION

InSAR is a proven tool for tracking large-scale time-varying surface deformation at active volcanoes, as exemplified by work at Etna, Italy [4,5]; Yellowstone, Wyoming [6,7]; Okmok, Alaska [8,9]; and many other locations around the world. ASAR-derived interferograms offer an excellent opportunity to track deformation of Hawaiian volcanoes because of the numerous look angles available over the island. As of early 2007, 27 independent look angles had been acquired, at least half of which cover some portion of Kīlauea volcano. Given ENVISAT's 35-day repeat cycle, this means that images of Kīlauea are collected about once every three days. The resulting wealth of spatially dense line-of-sight (LOS) displacement data from many different time periods provides an excellent view of changes in the spatial and temporal patterns of deformation over time.

Since the start of ASAR acquisitions over Hawai`i in early 2003, Kīlauea has undergone tremendous changes in the style and rate of summit deformation. Between the summers of 2003 and 2004, inflation was minor and localized within the summit caldera (Fig. 2, top). During the following year, the inflation broadened and the center shifted to the south, reflecting magma accumulation in a source about 3 km deep near the intersection of the east rift zone and summit caldera (Fig. 2, middle). During both of these time periods the southwest rift zone subsided, following the trend first noted by GPS in the mid-1990s. During summer 2005 to summer 2006, the inflation rate increased dramatically, shifted laterally to a source at 3-5 km depth beneath the south caldera (the site of the long-term magma reservoir [10]), and uplift characterized the upper southwest rift zone (Fig. 2, bottom). These changes appear to reflect an increase in the magma supply to Kīlauea volcano. In the years prior to 2003, subsidence dominated the summit region, supporting the inference that magma supply was balanced or exceeded by the eruption of lava from the Pu`u `Ō`ō vent [10]. The heightened 2005-2006 inflation rate was accompanied by an increase in the amount of magma that reached Pu`u `Ō`ō [11]; however, the increase in magma supply to the volcano must have been too large to be taken up by Pu`u `Ō`ō, causing the summit and southwest rift to inflate to accommodate the accumulation of magma.

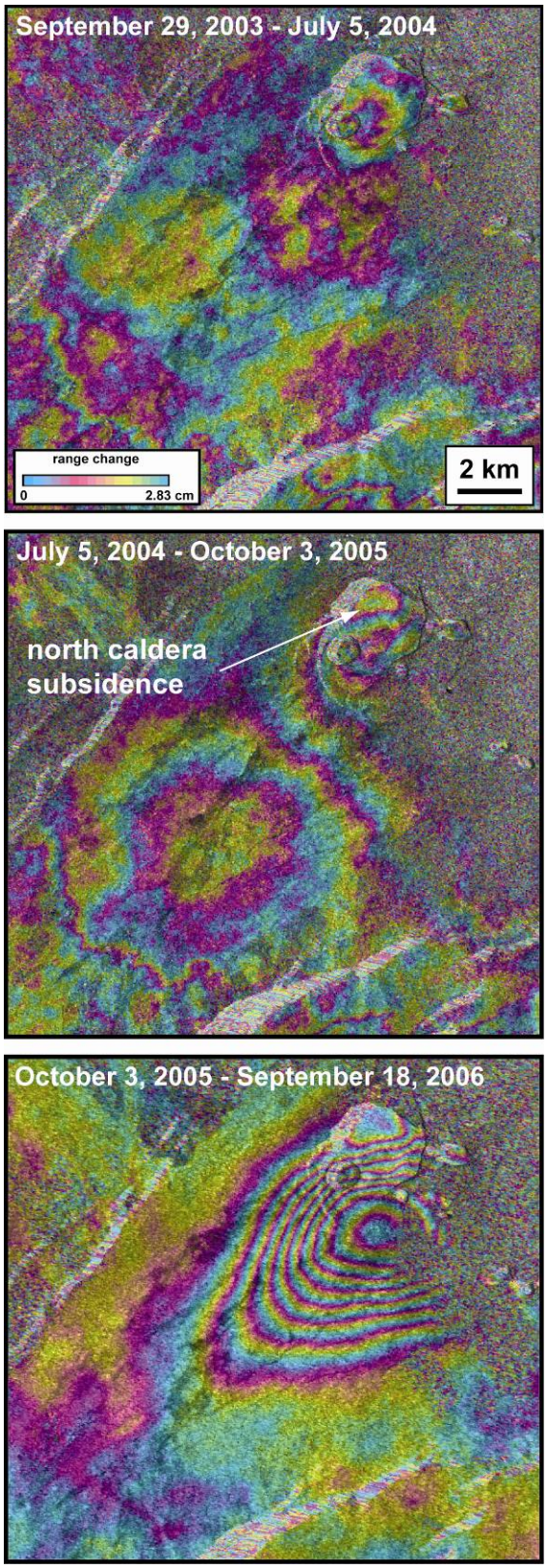

Figure 2. ASAR beam mode 2 track 200 interferograms showing deformation of the summit and southwest rift zone of Kīlauea volcano. Area covered by the figure is shown in Fig. 1.

Because of the current latency (usually between two and several weeks) between the acquisition of an ASAR scene of Hawai`i and processing at the Hawaiian Volcano Observatory, InSAR results from Kīlauea cannot be used for early detection of volcanic transients. Real- and near-real-time volcano monitoring will continue to be provided by ground-based continuous GPS, tilt, and seismic networks unless ASAR data can be made available in a more timely fashion. Radar interferograms do, however, offer guidance for additional monitoring and research efforts, and provide valuable contributions to the overall understanding of volcanic and tectonic events after their onset. For example, uplift along the southwest rift zone in 2006 was first detected by a single continuous GPS station, but the extent of the deformation was not realized until InSAR data were obtained.

3. LOCALIZED SUBSIDENCE DUE TO LAVA ACCUMULATION

Superimposed on the volcano-wide deformation of Kīlauea are several small (kilometer-scale) patches of subsidence. These patches are generally associated with recent accumulations of lava. For example, three subsiding areas on the east rift zone of the volcano are former pit craters that were filled by lava during the 1969-1974 eruption of Mauna Ulu (Fig. 3): Ala`e, `Ālo`i, and the east side of Makaopuhi (the latter was a nested pit crater until the deeper part was filled). Ala`e and Makaopuhi, being the larger of the three former pit craters, are subsiding at a faster rate (about 3-4 cm/yr LOS) than the smaller `Ālo`i (about 1 cm/yr). This means that Ala`e and Makaopuhi become incoherent in long-timespan interferograms, whereas fringes only become obvious around `Ālo`i in interferograms that span several years. In addition to the three filled pit craters, two recently active vents, Mauna Ulu (1969-1974) and Kupaianaha (1986-1992) are subsiding, probably also because both areas are the sites of thick accumulations of cooling and contracting lava. The Mauna Ulu, `Ālo`i, Ala`e, and Makaopuhi subsidence is overlain on larger-scale subsidence of the upper east rift zone (Fig. 3).

More mysterious is subsidence in the north part of Kīlauea caldera (Fig. 2, all three panels, labelled in the middle panel). Subsidence there of about 2 cm/yr LOS had not been detected prior to the application of InSAR because no terrestrial geodetic data (for example, leveling or GPS) had been collected there. No lava flows have been active in the north caldera region since 1919; thus, it seems unlikely that the deformation is caused by cooling and contraction of lava. During the mid-1800s, however, that part of the caldera hosted an active lava lake [12], so it is possible that the subsidence seen today reflects the location of a former vent structure beneath the caldera floor.

InSAR is the only technique that allows for rapid identification of such localized deformation sources, which is critical for terrestrial deformation monitoring. Methods like leveling and GPS rely upon point measurements from sometimes widely-spaced locations. Without the spatial resolution provided by InSAR, point measurements collected from these subsiding

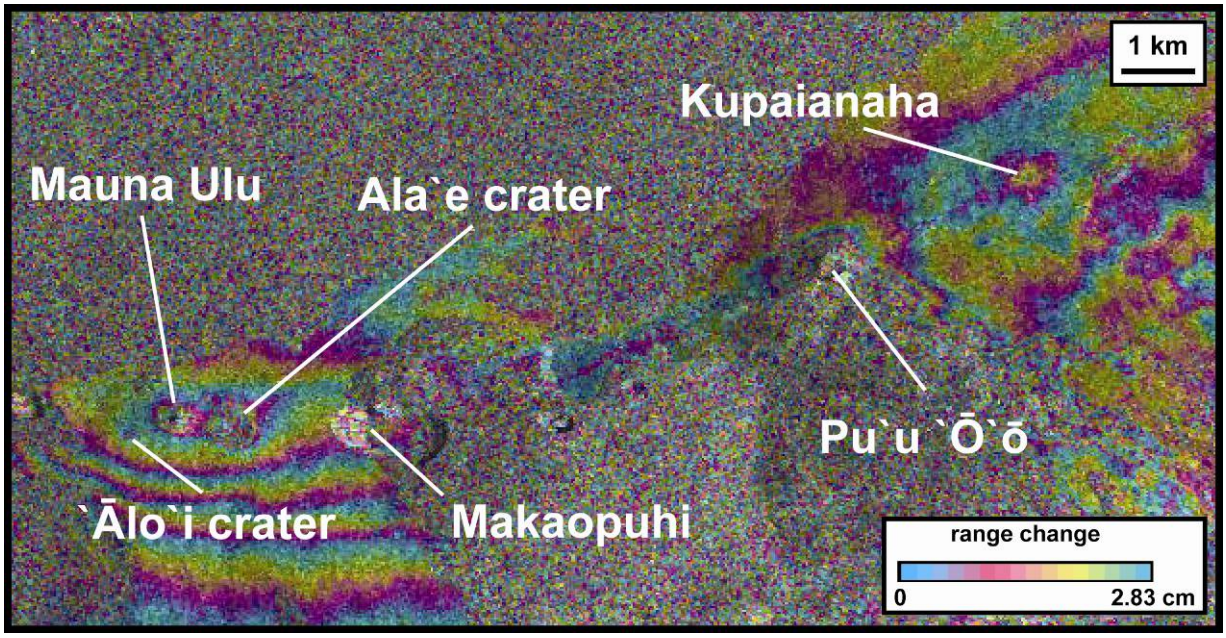

Figure 3. ASAR beam mode 2 track 429 interferogram spanning September 10, 2003 to February 21, 2007, showing deformation along Kīlauea's east rift zone. Labelled features are discussed in the text, and the area covered by the interferogram is given in Fig. 1.

accumulations of lava or former vent areas may be misinterpreted as reflecting other processes, leading to incorrect assessments of volcanic activity. By using the InSAR results as a guide, terrestrial geodetic monitoring can be designed to avoid such areas. Similar application of InSAR for geodetic network design and deployment was suggested for establishing GPS stations in the tectonically active southern California region, which experiences localized subsidence due to oil and groundwater extraction [13].

4. SURFACE INSTABILITY

Unlike the localized subsidence of accumulated lavas, which occurs at a relatively constant rate over time, surface instabilities start and stop in response to external stimuli. One such example of InSAR-detected surface instability is seaward motion of a portion of the coast above the East Lae`apuki lava delta, which formed at the point where a lava tube emptied into the ocean. A large delta at East Lae`apuki collapsed in November 2005, consuming 0.14 km^2 of delta and 0.04 km^2 of pre-existing land. Lava delta collapses are relatively common, owing to the instability of land formed at the lava-ocean interface, and the November 2005 collapse was the largest historic collapse to date.

InSAR results indicated that the area immediately adjacent to the collapse scarp began moving seaward at about 10 cm/month following the November 2005 collapse. The deformation is manifested in interferograms as a set of crescent-shaped fringes above the East Lae`apuki lava ocean entry (Fig. 4). GPS meas-

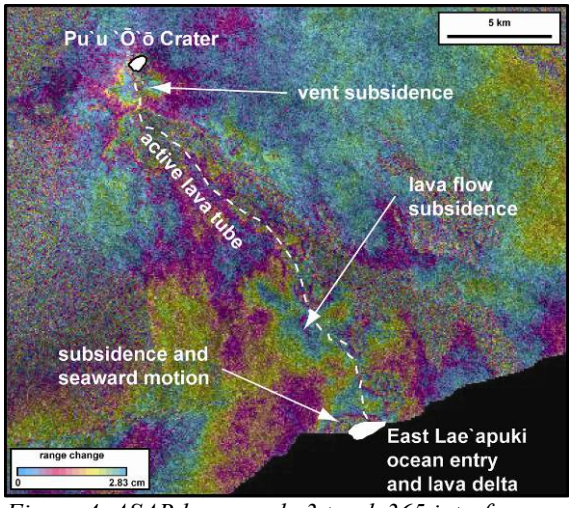

Figure 4. ASAR bean mode 3 track 365 interferogram spanning May 13 to September 30, 2006, and showing subsidence of recent lava flows and the vent region, as well as seaward motion of the coast above the lava delta (white area) caused by surface instability. Area covered by the image is shown in Fig. 1.

urements confirmed the displacement, and have shown that the rate of deformation has been relatively constant since the installation of the GPS instrument in November 2006. Based on the fact that the motion apparently started immediately after the November 2005 delta collapse, the most likely explanation is that the previously stable coast was disturbed by the removal of the lava delta. The spatial extent of the instability might indicate an area that is in danger of collapse if the new delta fails in the future.

5. LAVA FLOW MAPPING

As noted by previous workers, interferograms are incoherent where lava flows have covered the surface between radar scene acquisitions [8,14]. By tracking this incoherence, it is possible to map lava flow activity over time. Using InSAR data to track changes in the active flow field has the benefit of providing ~30 m spatial resolution while minimizing the amount of time required for field personnel to map flow margins using hand-held GPS units.

Coherence maps from Kīlauea's active flow field that span December 7, 2006 to March 22, 2007, illustrate the variations in lava flow activity over time, including the development of lava tubes. For example, during the entire time period spanned by Fig. 5, the lava entry into the ocean at location 1 was active (flows in the image are fed by a tube extending from Pu`u `Ō`ō to within 5-10 km of the coast). Between December 7, 2006, and January 11, 2007, the ocean entry was fed by surface lavas as indicated by incoherence (yellow area in Fig. 5 top) between the entry and the main area of lava flows. During January 11 to March 22, 2007, the area between the main flow and location 1 is coherent (blue color in Fig. 5 middle and bottom), indicating that no surface lavas were feeding the ocean entry. Since lava was still entering the ocean during this time period, a lava tube must have developed by January 11, 2007. A similar relation is apparent for ocean entry 2 during January 11 to March 22, 2007 (Fig. 5 middle and bottom). Although these relations may be obvious to observers on the ground, remote mapping of lava flow development provides an alternate means of tracking the evolution of the flow field, and would be especially useful at volcanoes that cannot be easily accessed by field personnel.

6. CONCLUSIONS

InSAR has provided a wealth of new insights into the deformation of Kīlauea volcano. ENVISAT ASAR

imagery has been used to track changes in the spatial and temporal pattern of volcano-wide deformation, identify previously unknown subsidence features, detect

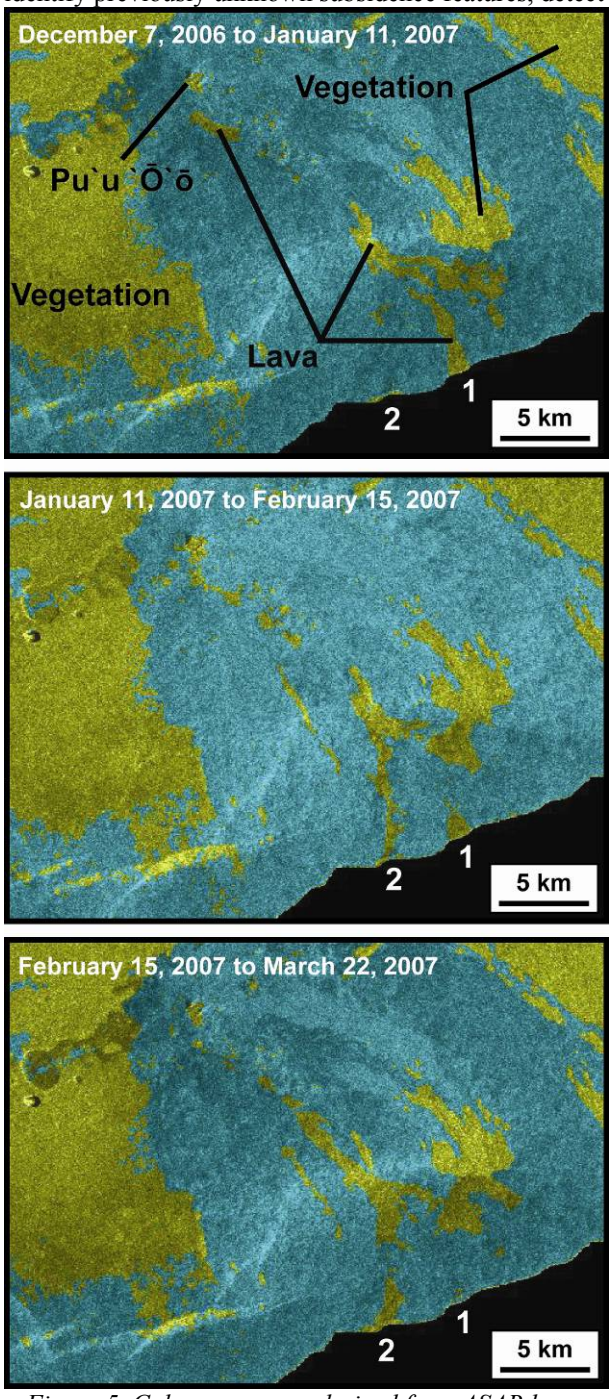

Figure 5. Coherence maps derived from ASAR beam mode 6 track 343 interferograms. Yellow areas have a coherence less than 0.3, and blue areas greater than 0.3. Area covered by the imagery is shown in Fig. 1.

the onset and evolution of surface instability, and map lava flow activity and lava tube development over time. Results of InSAR studies can be used to guide the deployment of terrestrial geodetic stations, and are stimulating exploration of new research directions. Future applications of InSAR to Hawai`i will build upon these results, especially using new sensors. C-band interferograms are generally incoherent where vegetation is dense, including the rain forests of Hawai`i. L-band sensors, however, can see through much of this vegetation, and offer promise for new insights into deformation of Kīlauea and other volcanoes.

7. ACKNOWLEDGEMENTS

ENVISAT ASAR data were provided by the European Space Agency as part of Cat-1 project 2765. Asta Miklius and Chuck Wicks provided helpful reviews.

8. REFERENCES

1. Kauahikaua, J., Cashman, K.V., Clague, D.A., Champion, D., and Hagstrum, J.T. (2002). Emplacement of the most recent lava flows on Hualalai Volcano, Hawai'i..*Bull. Volcanol.*, **64**(3-4), 229-253.
2. Decker, R.W., Klein, F.W. Okamura, A.T., and Okubo, P.G. (1995). Forecasting eruptions of Mauna Loa volcano, Hawaii. In *Mauna Loa Revealed* (Eds. J.M. Rhodes and J.P. Lockwood), AGU Geophysical Monograph 92, p. 337-348.
3. Heliker, C., and Mattox, T.N. (2003). The first two decades of the Pu`u `Ō`ō-Kupaianaha eruption: chronology and selected bibliography. In *The Pu`u `Ō`ō-Kupaianaha Eruption of Kīlauea Volcano, Hawai`i: The First 20 Years* (Eds. C. Heliker, D.A. Swanson, and T.J. Takahashi), U.S. Geological Survey Professional Paper 1676, p. 1-27.
4. Massonnet, D., Briole, P., and Arnaud, A. (1995). Deflation of Mount Etna monitored by spaceborne radar interferometry, *Nature* **375**(6532), 567-570.
5. Lundgren, P., Casu, F., Manzo, M., Pepe, A., Berardino, P., Sansosti, E., and Lanari, R. (2004). Gravity and magma induced spreading of Mount Etna Volcano revealed by satellite radar interferometry, *Geophys. Res. Let.* **31**(4), doi:04610.01029/02003GL018736.
6. Wicks Jr., C.W., Thatcher, W., and Dzurisin, D. (1998). Migration of fluids beneath Yellowstone Caldera inferred from satellite radar interferometry, *Science* **282**(5388), 458-462.
7. Wicks Jr., C.W., Thatcher, W., Dzurisin, D., and Svarc, J. (2006). Uplift, thermal unrest, and magma intrusion at Yellowstone caldera, *Nature* **440**(7080), 72-75.
8. Lu, Z., Mann, D., Freymueller, J.T., and Meyer, D.J. (2000). Synthetic aperture radar interferometry of Okmok volcano, Alaska: radar observations, *J. Geophys. Res.* **105**(B5), 10,791-710,806.
9. Lu, Z., Masterlark, T., and Dzurisin, D. (2005). Interferometric Synthetic Aperture Radar (InSAR)

Study of Okmok Volcano, Alaska, 1992-2003: Magma Supply Dynamics and Post-emplacement Lava Flow Deformation, *J. Geophys. Res.* **110**(B2), doi02410.01029/02004JB003148.

10. Cervelli, P.F., and Miklius, A. (2003). The shallow magmatic system of Kīlauea volcano. In *The Pu`u `Ō`ō-Kupaianaha Eruption of Kīlauea Volcano, Hawai`i: The First 20 Years* (Eds. C. Heliker, D.A. Swanson, and T.J. Takahashi), U.S. Geological Survey Professional Paper 1676, p. 149-163.
11. Elias, T., ad Sutton, A.J. (2007). Sulfur dioxide emission rates from Kīlauea volcano, Hawai`I, an update: 2002-2006. U.S. Geological Survey Open File Report 2007-1114.
11. Dutton, C.E. (2005). *Hawaiian Volcanoes*, University of Hawaii Press, Honolulu, pp 81-235.
12. Bawden, G.W., Thatcher, W., Stein, R.S., Hudnut, K.W., nad Peltzer, G. (2001). Tectonic contraction across Los Angeles after removal of groundwater pumping effects. *Nature* **412**(6849), 812-815.
13. Zebker, H.A., Rosen, P., Hensley, S., and Mouginis-Mark, P.J. (1996). Analysis of active lava flows on Kilauea Volcano, Hawaii, using SIR-C radar correlation measurements, *Geology*, **24**(6), 495-498.